EDGE ARTICLE

Symmetry-guided monomer design enables the combinatorial synthesis and targeted screening of polyesters

Xiaojie Feng,†[a] Xiaoying He,†[b] Jiayi Zhu,[b] Li-Hong Lin,[c] Qiaoyan Shang,[b] Zheng-Hong Luo, [c] Yin-Ning Zhou [*c] and Fangyou Yan [*a]

The rational design of polyester materials plays a crucial role in the development of functional polymers with tailored properties. In this work, we introduce a novel symmetry-guided molecular design strategy, which is a symmetry-aware, parameter-controlled design paradigm that both broadens and rationalizes the accessible chemical space of functional molecules. By introducing the concept of a pairwise atomic symmetry index (PASI) metric and applying targeted modifications to small molecules, a library of 10 614 diacids and 9983 diols is constructed, enabling a systematic and unexplored expansion of the chemical space of polyesters. The combinatorial pairing of these diacids and diols leads to the generation of over 100 million polyester structures. High-throughput prediction of the glass transition temperature (T_g) by the T_g-QSPR model aligns well with the typical thermal behavior in polyester materials. To validate the design methodology, a two-level verification process is performed. The predicted T_g values are first examined using molecular dynamics (MD) simulations and subsequently confirmed by differential scanning calorimetry experiments. The calculated T_g values show good agreement with both MD simulations (average absolute error (AAE) of 17.54 °C) and experimental measurements (AAE of 16.45 °C). These results further confirm the reliability and robustness of the proposed approach. This study not only provides an effective strategy for the large-scale generation of a polyester library and screening of property targeted polyesters, but also carries broader chemical implications beyond polyester design, offering potential insights for the development of functional molecules.

Introduction

Materials science is the cornerstone of human civilization, playing a fundamental and pioneering role in the development of science and technology. Polyester materials are a significant branch of polymer engineering and are widely used in various fields of life and production due to their excellent thermal stability, mechanical properties, and biodegradability. Examples include polymer electrolytes,[1–4] polymer membranes,[5–7] polymer dielectrics for flexible electronics,[8,9] self-healing polymers,[10–12] and high-temperature resistant materials.[13–16] However, the growing demand for high-performance and sustainable polyesters poses increasing challenges for traditional trial-and-error methods.

The emergence of polymer informatics has opened new opportunities for the expansion of polymers.[17–21] The rapid development of polymer informatics has led to research into the computer-aided design of high-performance polymers. Researchers can explore the relationship between the structure and properties (*e.g.*, thermal performances,[22–27] transfer performances,[28–33] electrical performances,[34–36] mechanical performances,[37–40] and optical performances[41–43]) of novel polymers to meet the needs of different fields.

Several frameworks have been developed to generate and evaluate polymers. Existing frameworks, such as the Open Macromolecular Genome (OMG)[44] and Small Molecules into Polymers (SMiPoly),[45] provide collections of commercially available or literature-derived monomers and define canonical polymerization pathways, enabling the construction of virtual polymer libraries. Generative models based on the Variational Autoencoder (VAE) framework[46] are accessible to the inverse design of polymers with targeted topologies and properties. High-throughput and data-driven strategies are also applied to accelerate the discovery of functional polymers. For example, Yu *et al.*[47] constructed a virtual space of over 100 000 polyimides and identified nine promising candidates for high-temperature energy storage through computational screening and molecular

aSchool of Chemical Engineering and Materials Science, Tianjin University of Science and Technology, Tianjin 300457, P.R. China. E-mail: yanfangyou@tust.edu.cn

bSchool of Marine and Environmental Science, Tianjin University of Science and Technology, Tianjin 300457, P.R. China

cState Key Laboratory of Synergistic Chem-Bio Synthesis, School of Chemistry and Chemical Engineering, Shanghai Jiao Tong University, Shanghai 200240, People's Republic of China. E-mail: zhouyn@sjtu.edu.cn

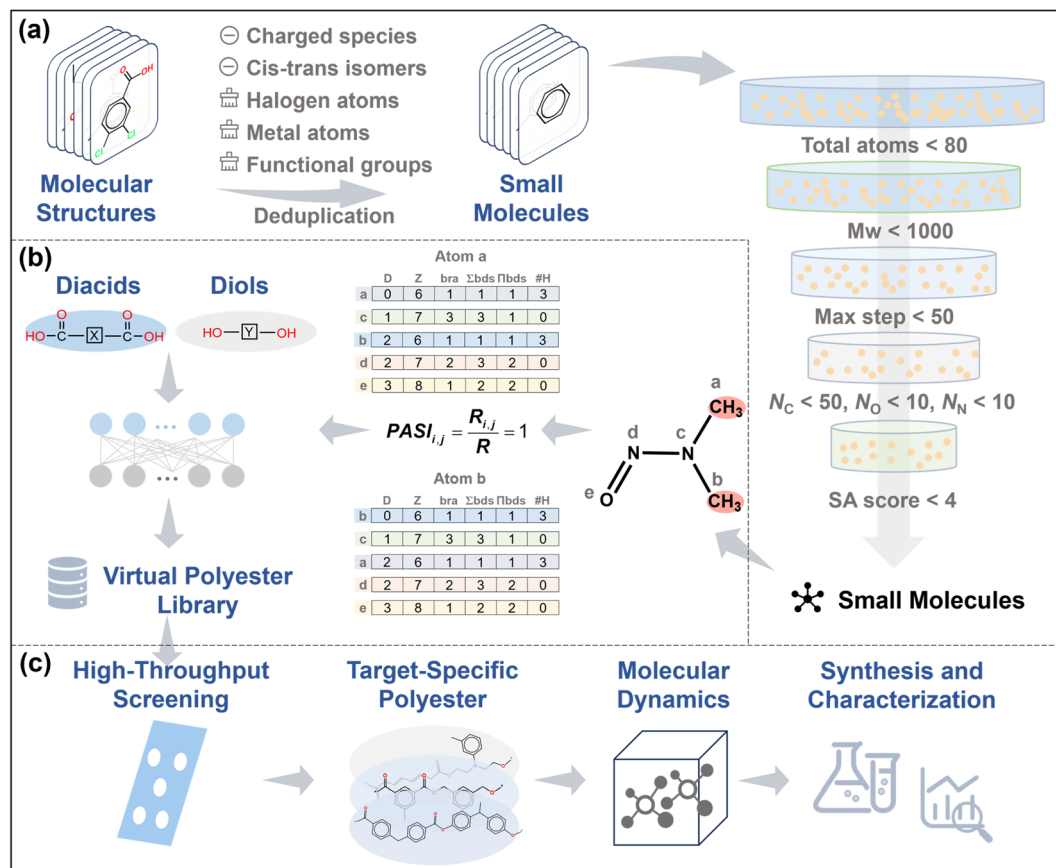† Both authors contributed equally to this work.

Fig. 1 Schematic illustration of this work. (a) Modification and screening of the initial molecular structures. (b) Calculation of PASI, generation of a virtual polyester library. (c) High-throughput screening of virtual polyesters, molecular dynamics, experimental synthesis, and characterization.

dynamics (MD) simulations. Similarly, He *et al.*[48] generated over 95 000 polyester candidates by combining diacids and diols and experimentally validated a quantitative structure–property relationship (QSPR) model for glass transition temperature (T_g).

Despite these advances, most current strategies rely mainly on retrosynthetic or combinatorial approaches, and systematic monomer design remains underexplored. To address this gap, we introduce a symmetry-guided monomer design strategy leveraging the pairwise atomic symmetry index (PASI) to guide the generation of novel monomers. By explicitly incorporating atomic-level symmetry constraints, this approach enables systematic exploration of polyester chemical space, providing a conceptual framework for rational polyester design that complements existing generative polymer methodologies.

Building on this conceptual framework, we apply the PASI-guided strategy to develop a practical monomer design workflow. In this study, we focus on small-molecule modification and use the T_g of polyesters as a case study to broaden the chemical space and enable targeted screening of polyesters (Fig. 1). First, small molecules for designing diacids and diols are obtained by systematically modifying the collected organic molecules. Second, the concept of PASI is introduced for the first time to address the issue of symmetry in atomic pairs within molecules. Guided by the PASI theory and incorporating the modified fragments, diacids and diols are designed

systematically. Subsequently, a library of hypothetical polyesters is generated through the enumeration of all possible diacid–diol combinations. To validate the design methodology, the T_g-QSPR model[48] is used to conduct a high-throughput screening of the virtual polyester library. Also, mechanistic or chemical insights are also provided according to the distribution of polyester T_g values along with their chemical structures. MD simulations and experimental validation are then performed. This design strategy not only enhances the efficiency of polyester design but also provides innovative ideas and methods for discovering polymer materials.

Results and discussion

Modification and screening of the initial molecular structures

First, the structures of more than 20 000 organic molecules are collected from the National Institute of Standards and Technology (NIST) database.[49] Owing to the complex structural features of some organic molecules, the organic structures are systematically modified according to the following rules (Fig. 1a): (1) exclusion of the charged species and *cis–trans* isomers; (2) removal of halogen atoms from organic molecules; (3) removal of metal atoms from organic molecules; (4) removal of intrinsic functional groups, including carboxyl, hydroxyl, ester, and amino groups; and (5) removal of duplicate small molecules. Furthermore, based on an analysis of the polyester
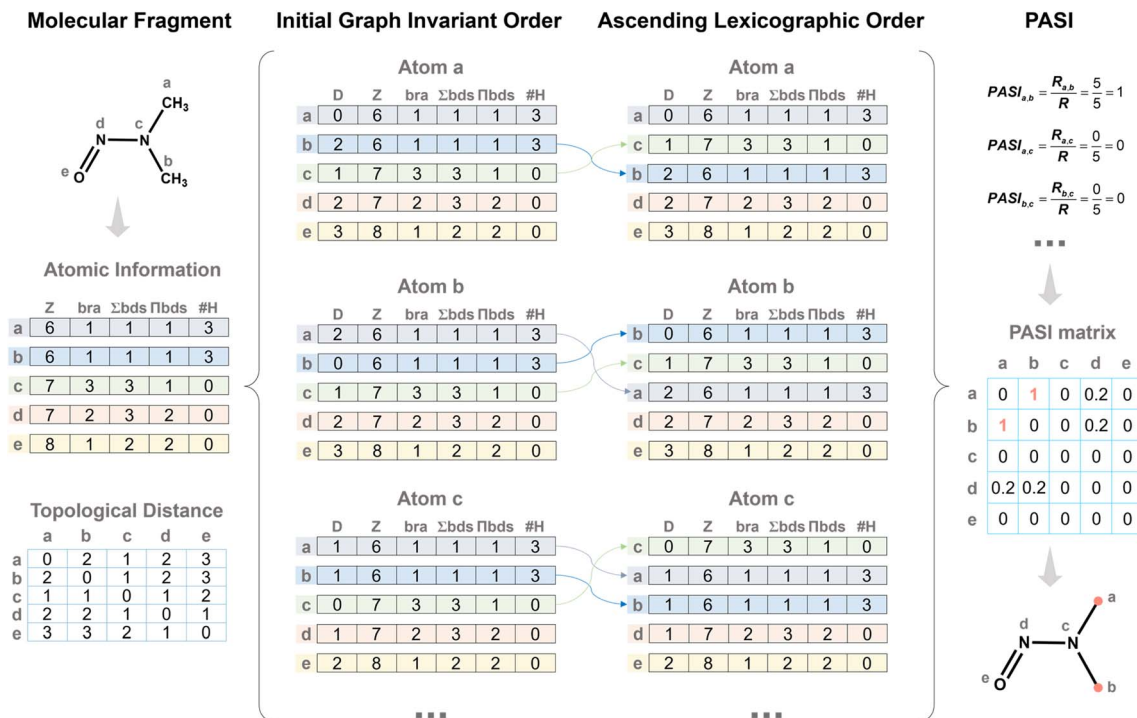
Fig. 2 Representative example illustrating the PASI.

database derived from PoLyInfo[50] (see the SI for details; Fig. S1), the modified molecules (H-suppressed structures) are further screened according to the following principles (Fig. 1a): (1) the total number of heavy atoms, defined as non-hydrogen atoms including carbon (C), nitrogen (N), oxygen (O), phosphorus (P), and sulfur (S), in small molecules <80; (2) the molecular weight of small molecules <1000; (3) the maximum step (*i.e.*, the longest topological distance) of small molecules <50; (4) the number of C atoms in small molecules <50; (5) the number of O atoms in small molecules <10; and (6) the number of N atoms in small molecules <10.

The synthetic accessibility score (SAscore) metric is used to assess the synthetic difficulty of a compound during the chemical synthesis process by analyzing its structural features.[51] Synthetic accessibility analysis enables researchers to screen and design substances more effectively, thereby enhancing the success rate and efficiency of novel material development. Generally, compounds with a lower SAscore are more readily synthesized, requiring relatively simpler reaction conditions and fewer synthetic steps. To reduce the synthetic complexity, 4116 small molecules with SAscores of less than 4.0 are selected for the subsequent design of polyester monomers. Detailed distribution information is provided in Fig. S2.

Pairwise atomic symmetry index (PASI)

Analysis of existing polyester monomers reveals that in most diacids and diols, the hydroxyl and carboxyl groups are located at symmetric positions. Based on this observation, the concept of the PASI is introduced to quantify the degree of symmetry between two atoms in a molecule (see the SI for details;

Algorithm S1). This facilitates the design of monomers with symmetry. The specific steps are as follows:

(1) Calculate the following for atom i: the topological distance (D)[52] between atom i and all atoms; the branched degree (bra); the sum of bond orders $(\sum bds)$, and the product of bond orders $(\prod bds)$. Additionally, record the atomic number (Z) and the number of bonded hydrogens (#H).

(2) The attribute tuples $(D, Z, bra, \sum bds, \prod bds, \#H)$ are sorted in ascending order following a lexicographic comparison scheme. Specifically, D is compared first; if entries have the same D value, Z is compared next, and the comparison proceeds sequentially through the remaining attributes. It should be noted that these attributes are treated as a set of parallel equivalence conditions rather than a weighted linear combination.

(3) Calculate the PASI between atoms i and j, as described in eqn (1).

$$\text{PASI}_{i,j} = \frac{R_{i,j}}{R} \tag{1}$$

where $R_{i,j}$ refers to the number of rows with identical information between atoms i and j after sorting in ascending order, and R represents the total amount of information, which is equal to the number of heavy atoms.

A representative example is provided to illustrate the PASI (Fig. 2). First, the atomic information $(Z, bra, \sum bd, \prod bds,$ and #H) for all atoms is obtained to construct the atomic information matrix. The D values between the atom and all other atoms are then computed, forming the initial matrix. Each matrix is sorted in ascending lexicographic order according to the sequence $(Z, bra, \sum bd, \prod bds,$ and #H). Finally, the sorted
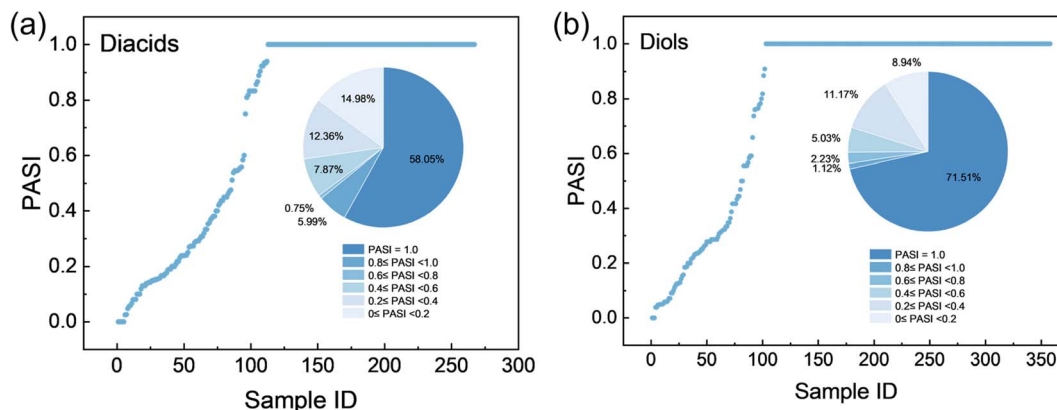
Fig. 3 Distributions of PASI values for (a) diacid and (b) diol sites in the monomer dataset (sourced from He *et al.*[48]).

matrices of two atoms are compared, and the ratio of identical rows to the total number of rows is defined as the PASI between the two atoms. In this example, atoms a and b have identical matrices, giving a PASI of 1.0, whereas atoms a and c share no identical rows, resulting in a PASI of 0. This example demonstrates how PASI quantitatively captures topological equivalence based on parallel atomic attributes.

Chemical space analysis

The virtual polyesters are produced by the condensation of diacids and diols. Analysis of the monomers (reported by He *et al.*[48]) derived from decomposing polyesters in the PolyInfo database shows that the majority of reactive functional groups are located at positions with PASI = 1.0 (Fig. 3). Specifically, 155 out of 267 diacids (58.05%) and 256 out of 358 diols (71.51%) have their –COOH and –OH groups located at PASI = 1.0, respectively. To prevent combinatorial explosion and ensure the simplicity and synthetic feasibility of the designed molecules, only atom pairs with a PASI of 1.0 (perfect symmetry) are used to introduce carboxyl and hydroxyl groups to generate diacid and diol molecules. In addition, it is stipulated that the maximum step between symmetric points with a PASI of 1.0 should be greater than 0.3 times the maximum step of the small molecule to prevent the monomer molecules from having excessively long side chains. Finally, a total of 10 614 diacids and 9983 diols are successfully designed by introducing carboxyl and hydroxyl groups at the symmetric positions. Comprehensive details are provided in the SI (Data.xlsx). The diacids are labeled as A1-A10614, while the diols are marked as B1-B9983. Although constraining the design to PASI = 1.0 reduces the design space, this is an intentional and adjustable choice. The PASI enables quantitative control of atomic-level topological symmetry,

allowing the design space to be flexibly expanded or contracted according to the application.

In terms of data scale and chemical diversity, the diacid and diol monomers included in several representative frameworks are compared, as summarized in Table 1. SMiPoly[45] collected 1083 small molecules extracted from the literature, including 81 diacids and 63 diols, whereas OMG[44] screened 3.1 million molecules from the eMolecules database and identified 1911 diacids and 6581 diols. In this work, the PASI-guided design strategy generates 10 614 diacids and 9983 diols. Fig. 4a illustrates the visualization of the Morgan fingerprint feature (radius = 2, fpSize = 2048) for diacids and diols, respectively, obtained using the t-distributed stochastic neighbor embedding (t-SNE) algorithm.[53–55] Compared to the existing methods, this work spans a broader chemical space. It highlights that our method introduces a symmetry-aware, parameter-controlled design paradigm that both broadens and rationalizes the accessible chemical space.

Additionally, the PASI-guided monomers were evaluated by searching the designed diacids and diols in the PubChem database (https://pubchem.ncbi.nlm.nih.gov/), which contains 122 million compounds. The results show that 77.9% of the designed diacids and 67.8% of the designed diols are not present in PubChem, indicating high novelty. These findings confirm that PASI-guided selection effectively explores previously unreported chemical space.

Furthermore, Fig. 4b shows the molecular weight distribution of the diacids and diols. The molecular weight of the diacids is primarily concentrated in the range of 150 to 540 g mol^{-1}, while the molecular weight of the diols is mainly distributed between 120 and 480 g mol^{-1}. Ring atom distributions (Fig. 4c and d) reveal that over 60% of monomers contain cyclic substructures, with the ratio of ring atoms to heavy atoms (RA/HA) values spanning a wide range. This variability allows systematic tuning of polyester properties. For example, lower RA/HA values enhance flexibility and processability, while higher RA/HA values improve rigidity and thermal stability. Fig. 4e shows that the SAscores of both the diacids and diols are concentrated between 1.7 and 4.0, indicating that the synthesis of the designed diacids and diols is acceptable and feasible under certain conditions and thus accelerate synthesis.

Table 1 Comparison of diacid and diol datasets with references

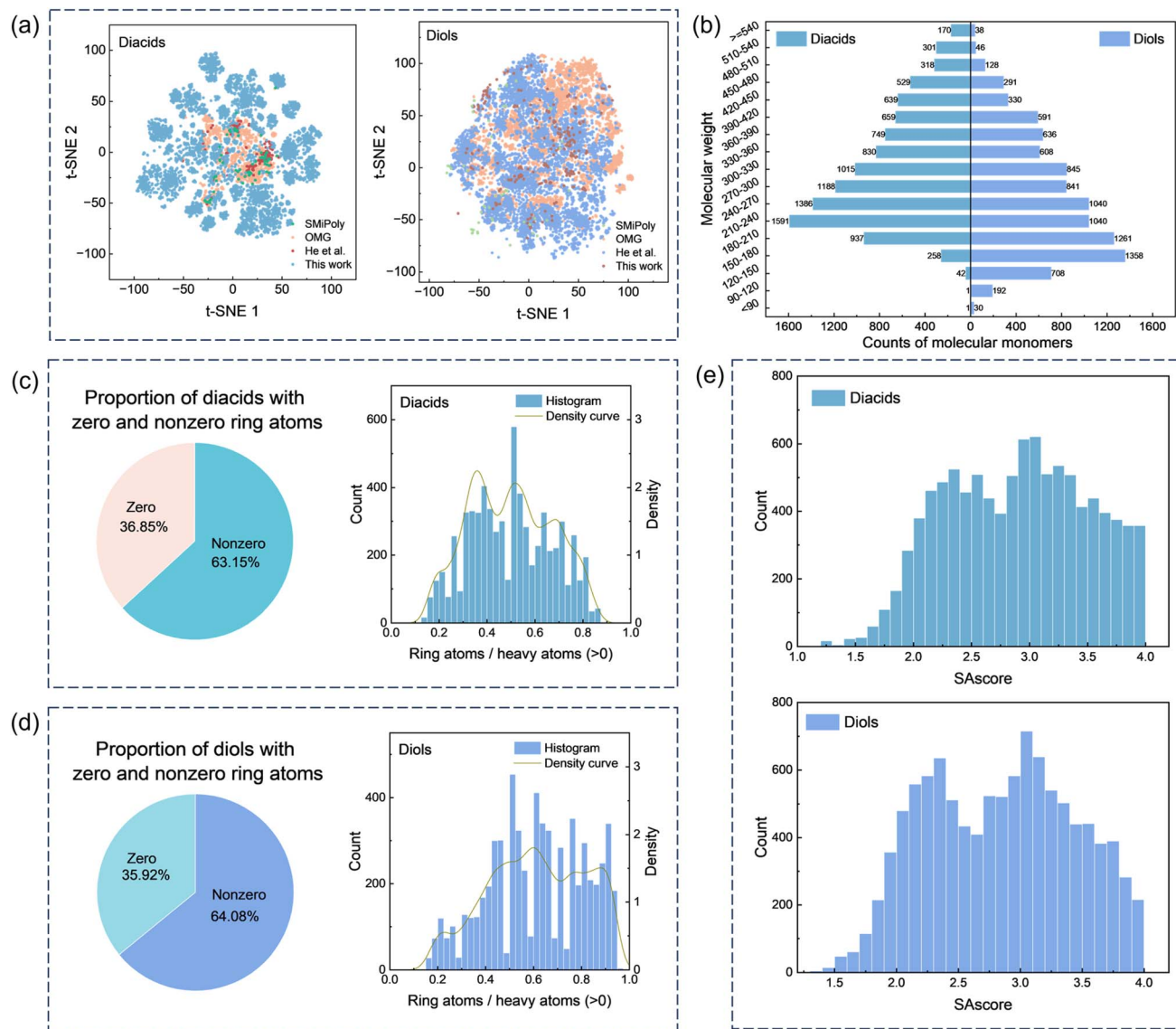| Method	Diacids	Diols
SMiPoly[45]	81	63
OMG[44]	1911	6581
He *et al.*[48]	267	358
This work	10 614	9983

Fig. 4 Information on the designed diacids and diols. (a) Chemical space visualization of the designed diacids and diols in datasets OMG,[44] SMiPoly,[45] He et al.,[48] and this work. (b) Counts of the designed diacids and diols across different molecular weight ranges. (c) Distribution of ring atom ratios in the designed diacid molecules. (d) Distribution of ring atom ratios in the designed diol molecules. (e) Distribution histogram of the SAscore of the designed diacids and diols.

Finally, over 100 million virtual polyester molecules are successfully generated utilizing computational methods to identify characteristic functional groups, such as carboxyl (–COOH) and hydroxyl (–OH) groups, within the simplified molecular input line entry system (SMILES) of the monomer. In the future, one can also adopt symmetry constraints with extra expert knowledges as new design principles to control physicochemical properties of polymers (e.g., controlling chain rigidity or crystallinity).

High-throughput screening of polyesters

Employing the validated T_g-QSPR model[48] (eqn (2)) to calculate the T_g of over 100 million virtual polyester molecules represented by $A_i\_B_j$ provides an initial assessment of their thermal stability.

$$T_g = \sum_{i=1}^{8} b_i \times I_i + \frac{1}{\max(\mathrm{MS_F})} \sum_{i=9}^{14} b_i \times I_i$$

$$+ \frac{1}{\sqrt{\sum_i \sum_j \mathrm{MS_F}}} \sum_{i=15}^{15} b_i \times I_i + \frac{1}{n_A} \sum_{i=16}^{20} b_i \times I_i$$

$$+ \frac{1}{n_{nH}} \sum_{i=21}^{29} b_i \times I_i - 1468.96278$$

$$n = 695; R^2 = 0.9060;$$

$$Q_{\mathrm{LOO-CV}}^2 = 0.8889; \mathrm{AAE} = 17.7197 \,^{\circ}\mathrm{C} \tag{2}$$

where n_A is the number of atoms, n_{nH} is the number of non-hydrogen atoms, and $\mathrm{MS_F}$ is a full-step matrix calculated from the polyester structures (H-suppressed).
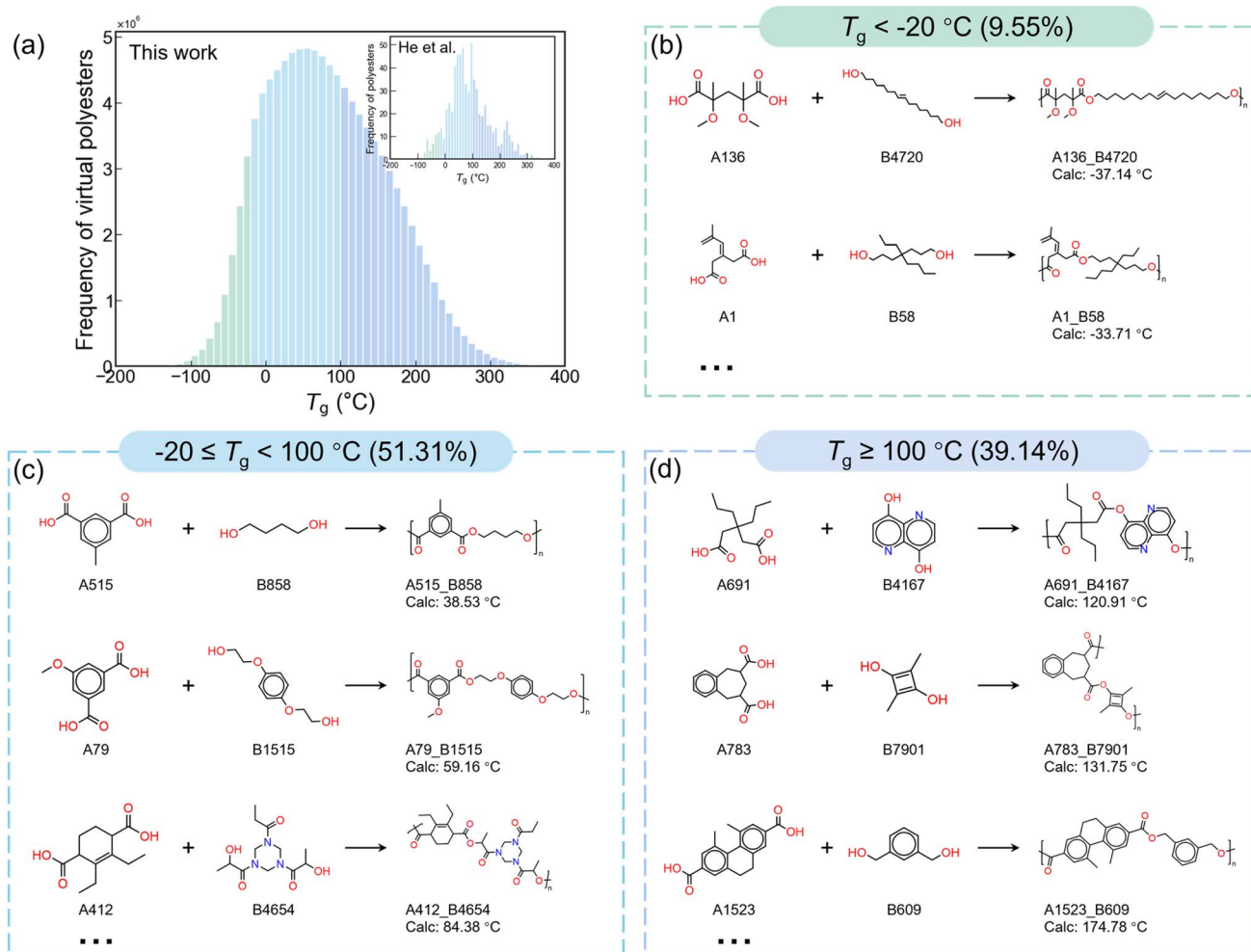
Fig. 5   Distribution of polyester T_g values and representative samples across different T_g ranges. (a) Distribution histogram of the polyester T_g values. (b) Several polyester samples with low T_g values ($T_g < -20$ °C). (c) Several polyester samples with medium T_g values ($-20 \leq T_g < 100$ °C). (d) Several polyester samples with high T_g values ($T_g > 100$ °C).

Fig. 5a presents the distribution histogram of the polyester T_g values. This distribution trend aligns with the typical thermal stability characteristics of polyester materials (He et al.[48]), suggesting that this design strategy is feasible and effective. It is worth noting that there are also T_g values beyond the plotted range (−200 °C to 400 °C): 0.0189% polyesters have T_g values below −200 °C, and 0.005% have values above 400 °C. Such extreme values are likely due to model-induced deviations when operating outside its applicable domain. Fig. 5b–d show representative polyester samples selected from different T_g ranges. Analysis of these structures reveals a clear trend that polyesters with higher T_g values typically contain a higher fraction of cyclic units (e.g., aromatic or alicyclic rings), whereas those with lower T_g values generally contain fewer ring units and often feature longer aliphatic chains. This behavior arises from the intrinsic rigidity of cyclic groups, which restricts local segmental mobility and consequently increases the T_g. In contrast, longer aliphatic chains increase conformational flexibility and enhance segmental mobility, ultimately leading to lower T_g values. In addition, several representative T_g values of commonly used commercial polyesters from open reports and

model predictions are listed in Table S1 to provide a reference for the T_g range of the designed polyesters.

Molecular dynamics simulations

MD simulations are conducted to preliminarily assess the reliability of the screening results derived from the T_g-QSPR model. All molecular simulations were performed using the polymer consistent force field (PCFF)[56,57] within the LAMMPS program.[58,59] Details of the dynamics simulation procedure are provided in the SI.

A total of 19 polyesters (Fig. 6a and b) were selected based on their predicted T_g values, which are randomly distributed within the range of −80 °C to 180 °C. This ensures that the MD validation covers a broad chemical space. The detailed MD simulation results are provided in Fig. S3 in the SI. Fig. 6c shows the correlation between the T_g values obtained from MD simulations and those predicted by the T_g-QSPR model. The shaded region represents the convex hull of the T_g-QSPR model. All MD data points fall within this convex hull, indicating that the MD predictions are consistent with the reasonable
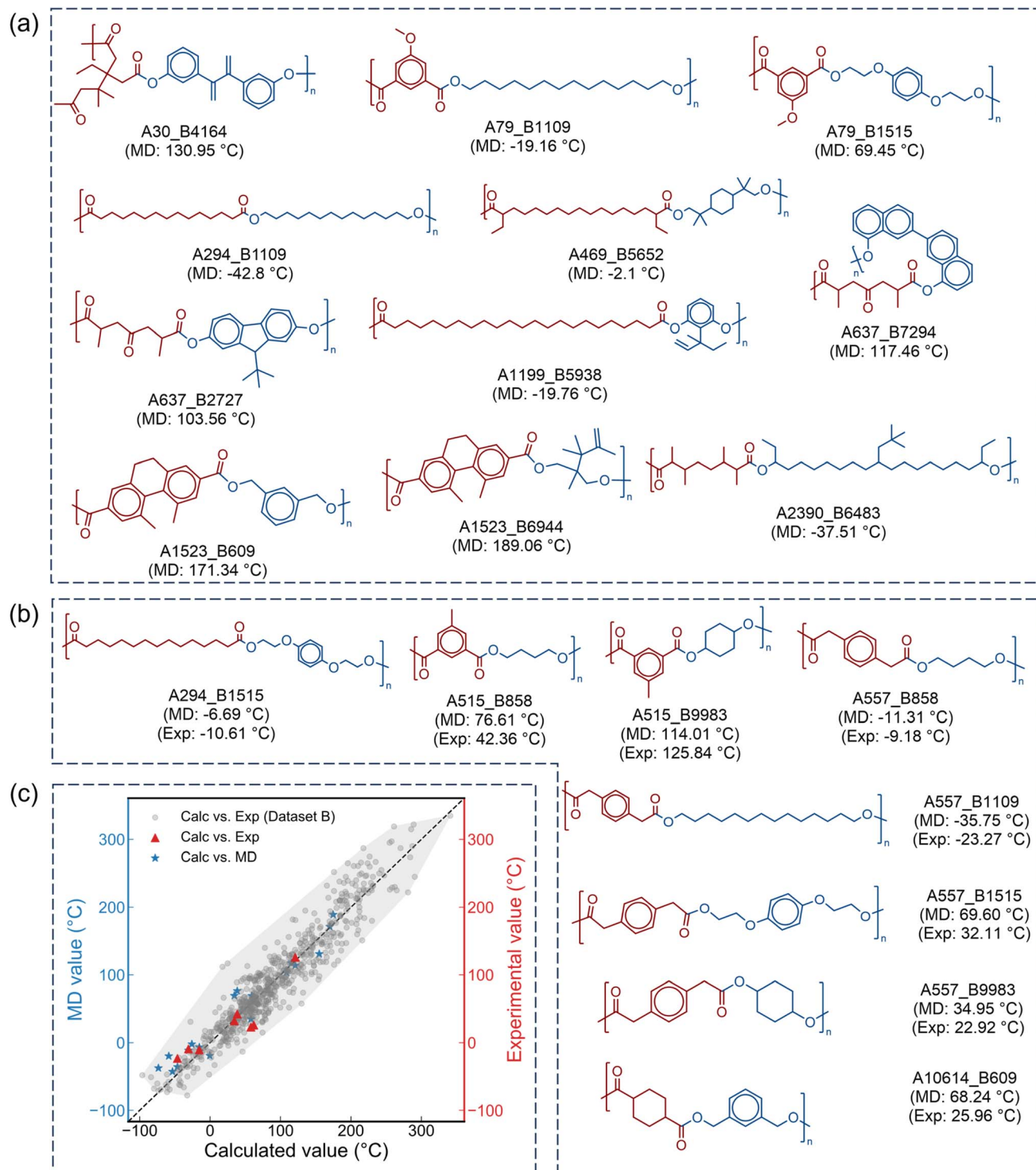
Fig. 6 Summary of MD simulations and experimental validation. (a) Polyester structures with only MD simulations. (b) Polyester structures with both MD simulations and experimental validation. (c) A comparison of the calculated T_g, MD-predicted T_g, and experimental T_g, with Dataset B sourced from He *et al.*[48]

distribution domain of the T_g-QSPR model and further confirming the rationality of the design strategy. The maximum absolute error (AE$_{max}$, SI eqn (S1)) is 38.94 °C, and the average absolute error (AAE, SI eqn (S2)) is 17.54 °C, closely matching the model's AAE (17.72 °C). These findings suggest that the selected polyesters preliminarily exhibit the targeted thermal

properties. It should be noted that, as not all PCFF parameters are directly available in LAMMPS, missing terms are generated using the automated conversion script insight2lammps.pl (https://www.MatSci.org). This process may result in minor deviations in bond-angle or torsional parameters, which can have a slight impact on the MD-predicted T_g values.

Experimental synthesis and characterization of polyesters

To experimentally validate the T_g values predicted by the T_g-QSPR model and corroborated by MD simulations, a subset of the selected polyesters was synthesized and characterized by differential scanning calorimetry (DSC) measurements. For the experimentally relevant polyesters, the diacid or diol components were confirmed to be absent from the dataset reported by He *et al.*,[48] ensuring that the resulting polyesters represent new structures. Details of the experimental procedures and the corresponding DSC curves are available in the SI (Fig. S4).

Fig. 6c illustrates a comparison of the calculated T_g values (Calc.), MD-predicted T_g values, and experimental T_g values (Exp.). Similarly, all experimental data points fall within the convex hull. The AE_{max} between the Calc. and Exp. values is 36.02 °C, with an AAE of 16.45 °C. A similar consistency is observed between the MD and Exp. values (AE_{max} of 42.25 °C and AAE of 19.55 °C). These results demonstrate that the T_g-QSPR model produces consistent results with both experimental measurements and MD simulations. They further confirm the effectiveness of the proposed polyester design strategy, providing a reliable approach to the high-throughput screening and rational design of polyesters with the desired thermal properties.

Limitations and future directions

It should be noted that the PASI method primarily addresses molecular symmetry at the level of topological structures. Three-dimensional geometric symmetry and electronic symmetry are not considered in the current implementation. Additionally, this study focuses on the synthetic feasibility of the monomers, whereas a systematic evaluation of the polyesters' synthetic accessibility is not conducted. The synthetic accessibility of actual polyesters may still be influenced by factors such as melting point, boiling point, and monomer compatibility. These limitations point to important directions for future work, including the integration of three-dimensional and electronic symmetry information to further enhance the accuracy and reliability of polyester design, as well as the systematic assessment of polyester synthetic feasibility to accelerate their production.

Conclusion

This work proposes a symmetry-aware, parameter-controlled design paradigm that both broadens and rationalizes the accessible chemical space of functional molecules. The PASI metric enables quantitative control over atomic-level topological symmetry, allowing the design space to be flexibly expanded or contracted according to the specific application. As a demonstration purpose, a rational framework for constructing symmetric diacid and diol monomers with PASI = 1.0 was illustrated through the modification of small molecules with SAscores <4.0, resulting in 10 614 diacids and 9983 diols with SAscores ranging from 1.7 to 4.0.

Combinatorial enumeration of these designed diacids and diols generated over 100 million polyester structures, greatly enriching the diversity of candidate materials. A high-throughput evaluation of the T_g across the designed polymer library reveals a consistent trend with the typical thermal behavior observed in polyester materials. This statistical trend supports the effectiveness of the proposed monomer-design based methodology. Furthermore, the strategy was validated through a two-level verification process, in which the T_g values predicted by the T_g-QSPR model were first examined by MD simulations and subsequently confirmed by DSC experiments. The calculated T_g values show good agreement with both MD simulations (AE_{max} of 38.94 °C and AAE of 17.54 °C) and experimental measurements (AE_{max} of 36.02 °C and AAE of 16.45 °C). This consistency further confirms the reliability and robustness of the design approach that significantly expands the chemical space of polyesters. The expanded polyester library is expected to accelerate real-world polymer discovery and enable the development of high-performance materials for packaging, biomedical devices, and sustainable plastics.

It is worth emphasizing that diacids and diols, as highly reactive key intermediates, play an important role in the construction of complex organic molecules such as drug compounds and fine chemicals. Therefore, this strategy also carries broader chemical implications beyond polyester design, offering potential insights for the development of functional molecules.

Author contributions

F. Y. Y and Y.-N. Z. conceived the problem. X. J. F. and X. Y. H. carried out detailed studies. X. J. F., X. Y. H., J. Y. Z., F. Y. Y and Y.-N. Z. analyzed the problem and designed the method. X. J. F. L. H. L and Q. Y. S co-analyzed the results. X. J. F. wrote the manuscript and F. Y. Y and Y.-N. Z. made modifications. Z. H. L. provided strategic guidance. All authors contributed to useful discussions.

Conflicts of interest

There are no conflicts to declare.

Data availability

The Python codes supporting the findings of this study are publicly available from GitHub (https://github.com/FangyouYan/PairwiseAtomicSymmetryIndex). The repository includes the LAMMPS input files, force–field parameters, and Python scripts used for PASI calculation. In addition, the predicted T_g of the virtual polyesters are available on Zenodo (https://zenodo.org/records/17627401).

Supplementary information (SI): additional results. See DOI: https://doi.org/10.1039/d5sc07720f.

Acknowledgements

References

1 X.-Y. Huang, C.-Z. Zhao, W.-J. Kong, N. Yao, Z.-Y. Shuang, P. Xu, S. Sun, Y. Lu, W.-Z. Huang, J.-L. Li, L. Shen, X. Chen, J.-Q. Huang, L. A. Archer and Q. Zhang, *Nature*, 2025, **646**, 343–350.

2 R. K. Gautam, X. Wang and J. J. Jiang, *Nat. Commun.*, 2025, **16**, 8830.

3 S. Liu, W. Liu, D. Ba, Y. Zhao, Y. Ye, Y. Li and J. Liu, *Adv. Mater.*, 2023, **35**, 2110423.

4 J. Chen, C. He, X. Peng, J. Li, X. Xu, Y. Zhou, J. Shen, J. Sun, Y. Li and T. Zhao, *Nat. Commun.*, 2025, **16**, 8494.

5 M. Sandru, E. M. Sandru, W. F. Ingram, J. Deng, P. M. Stenstad, L. Deng and R. J. Spontak, *Science*, 2022, **376**, 90–94.

6 C. Fan, H. Wu, J. Guan, X. You, C. Yang, X. Wang, L. Cao, B. Shi, Q. Peng, Y. Kong, Y. Wu, N. A. Khan and Z. Jiang, *Angew. Chem., Int. Ed.*, 2021, **60**, 18051–18058.

7 M. J. Baran, M. E. Carrington, S. Sahu, A. Baskin, J. Song, M. A. Baird, K. S. Han, K. T. Mueller, S. J. Teat, S. M. Meckler, C. Fu, D. Prendergast and B. A. Helms, *Nature*, 2021, **592**, 225–231.

8 G. Lee, S. C. Jang, J. H. Lee, J.-M. Park, B. Noh, H. Choi, H. Kweon, D. H. Kim, H. Y. Kim, H.-S. Kim and K. J. Lee, *Adv. Funct. Mater.*, 2024, **34**, 2405530.

9 J.-H. Lee, K. Cho and J.-K. Kim, *Adv. Mater.*, 2024, **36**, 2310505.

10 J. Jing, B. Yao, W. Sun, J. Chen, J. Xu and J. Fu, *Angew. Chem., Int. Ed.*, 2024, **63**, e202410693.

11 M. Chi, L. Sun, M. Nishiura, L. Huang, H. Zhang, Y. Higaki, S. Lee, K. Fukuda, Y. Zhao, T. Someya and Z. Hou, *J. Am. Chem. Soc.*, 2025, **147**, 23128–23135.

12 C. C. M. Sproncken, P. Liu, J. Monney, W. S. Fall, C. Pierucci, P. B. V. Scholten, B. Van Bueren, M. Penedo, G. E. Fantner, H. H. Wensink, U. Steiner, C. Weder, N. Bruns, M. Mayer and A. Ianiro, *Nature*, 2024, **630**, 866–871.

13 T. Luo, C. Lu, J. Qi, C. Wang, F. Chu and J. Wang, *Chem. Eng. J.*, 2024, **479**, 147729.

14 W. Xu, C. Zhou, W. Ji, Y. Zhang, Z. Jiang, F. Bertram, Y. Shang, H. Zhang and C. Shen, *Angew. Chem., Int. Ed.*, 2024, **63**, e202319766.

15 Z. Xu, M. Zhao, Z. Yang, P. Wang, J. Liu, Y. Xie, Y. Wu, M. Gao, L. Li, X. Song and C. Dai, *Adv. Funct. Mater.*, 2024, **34**, 2405111.

16 R. Wang, Y. Zhu, S. Huang, J. Fu, Y. Zhou, M. Li, L. Meng, X. Zhang, J. Liang, Z. Ran, M. Yang, J. Li, X. Dong, J. Hu, J. He and Q. Li, *Nat. Mater.*, 2025, **24**, 1074–1081.

17 A. Jayaraman and B. Olsen, *Macromolecules*, 2024, **57**, 7685–7688.

18 L. Chen, G. Pilania, R. Batra, T. D. Huan, C. Kim, C. Kuenneth and R. Ramprasad, *Mater. Sci. Eng.: R: Rep.*, 2021, **144**, 100595.

19 L. Gao, J. Lin, L. Wang and L. Du, *Acc. Mater. Res.*, 2024, **5**, 571–584.

20 W. Ge, R. De Silva, Y. Fan, S. A. Sisson and M. H. Stenzel, *Adv. Mater.*, 2025, **37**, 2413695.

21 P. L. Jacob, M. I. Parker, D. J. Keddie, V. Taresco, S. M. Howdle and J. Hirst, *Chem. Sci.*, 2025, DOI: 10.1039/D5SC05380C.

22 S. Wu, Y. Kondo, M.-a. Kakimoto, B. Yang, H. Yamada, I. Kuwajima, G. Lambard, K. Hongo, Y. Xu, J. Shiomi, C. Schick, J. Morikawa and R. Yoshida, *npj Comput. Mater.*, 2019, **5**, 66.

23 L. Tao, J. He, N. E. Munyaneza, V. Varshney, W. Chen, G. Liu and Y. Li, *Chem. Eng. J.*, 2023, **465**, 142949.

24 L. Tao, G. Chen and Y. Li, *Patterns*, 2021, **2**, 100225.

25 S. Zhang, S. Du, L. Wang, J. Lin, L. Du, X. Xu and L. Gao, *Chem. Eng. J.*, 2022, **448**, 137643.

26 H. Qiu, J. Wang, X. Qiu, X. Dai and Z.-Y. Sun, *Macromolecules*, 2024, **57**, 3515–3528.

27 J. Xu and T. Luo, *npj Comput. Mater.*, 2024, **10**, 74.

28 J. W. Barnett, C. R. Bilchak, Y. Wang, B. C. Benicewicz, L. A. Murdock, T. Bereau and S. K. Kumar, *Sci. Adv.*, 2020, **6**, eaaz4301.

29 M. Wang, Q. Xu, H. Tang and J. Jiang, *ACS Appl. Mater. Interfaces*, 2022, **14**, 8427–8436.

30 J. Yang, L. Tao, J. He, J. R. McCutcheon and Y. Li, *Sci. Adv.*, 2022, **8**, eabn9545.

31 M. Yang, J.-J. Zhu, A. L. McGaughey, R. D. Priestley, E. M. V. Hoek, D. Jassby and Z. J. Ren, *Environ. Sci. Technol.*, 2024, **58**, 10128–10139.

32 B. K. Phan, K.-H. Shen, R. Gurnani, H. Tran, R. Lively and R. Ramprasad, *npj Comput. Mater.*, 2024, **10**, 186.

33 J. Xu, A. Suleiman, G. Liu, M. Perez, R. Zhang, M. Jiang, R. Guo and T. Luo, *Cell Rep. Phys. Sci.*, 2024, **5**, 102067.

34 L. Chen, C. Kim, R. Batra, J. P. Lightstone, C. Wu, Z. Li, A. A. Deshmukh, Y. Wang, H. D. Tran, P. Vashishta, G. A. Sotzing, Y. Cao and R. Ramprasad, *npj Comput. Mater.*, 2020, **6**, 61.

35 R. Wang, Y. Zhu, J. Fu, M. Yang, Z. Ran, J. Li, M. Li, J. Hu, J. He and Q. Li, *Nat. Commun.*, 2023, **14**, 2406.

36 P. Xu, T. Lu, L. Ju, L. Tian, M. Li and W. Lu, *J. Phys. Chem. B*, 2021, **125**, 601–611.

37 X. Liang, X. Zhang, L. Zhang, L. Liu, J. Du, X. Zhu and K. M. Ng, *Ind. Eng. Chem. Res.*, 2019, **58**, 15542–15552.

38 Y. Hu, W. Zhao, L. Wang, J. Lin and L. Du, *ACS Appl. Mater. Interfaces*, 2022, **14**, 55004–55016.

39 T. Yue, J. He, L. Tao and Y. Li, *J. Chem. Theory Comput.*, 2023, **19**, 4641–4653.

40 W. Guo, S. Chai, L. Zhang and J. Du, *Chem. Ing. Tech.*, 2023, **95**, 447–457.

41 S. Zhang, X. He, P. Xiao, X. Xia, F. Zheng, S. Xiang and Q. Lu, *Adv. Funct. Mater.*, 2024, **34**, 2409143.

42 A. Mishra, P. Rajak, A. Irie, S. Fukushima, R. K. Kalia, A. Nakano, K.-i. Nomura, F. Shimojo and P. Vashishta, *Appl. Phys. Lett.*, 2023, **123**, 121901.

43 J. Najeeb, S. S. A. Shah, M. H. Tahir, A. I. Hanafy, S. M. El-Bahy and Z. M. El-Bahy, *Mater. Chem. Phys.*, 2024, **324**, 129685.

44 S. Kim, C. M. Schroeder and N. E. Jackson, *ACS Polym. Au*, 2023, **3**, 318–330.

45 M. Ohno, Y. Hayashi, Q. Zhang, Y. Kaneko and R. Yoshida, *J. Chem. Inf. Model.*, 2023, **63**, 5539–5548.

46 S. Jiang, A. B. Dieng and M. A. Webb, *npj Comput. Mater.*, 2024, **10**, 139.

47 M. Yu, Q. Jia, Q. Wang, Z.-H. Luo, F. Yan and Y.-N. Zhou, *Chem. Sci.*, 2024, **15**, 18099–18110.

48 X. He, M. Yu, J.-P. Han, J. Jiang, Q. Jia, Q. Wang, Z.-H. Luo, F. Yan and Y.-N. Zhou, *AIChE J.*, 2024, **70**, e18409.

49 NIST Chemistry WebBook, NIST Standard Reference Database Number 69, https://webbook.nist.gov/chemistry/.

50 M. Ishii, T. Ito, H. Sado and I. Kuwajima, *Sci. Technol. Adv. Mater.: Methods*, 2024, **4**, 2354649.

51 P. Ertl and A. Schuffenhauer, *J. Cheminform.*, 2009, **1**, 8.

52 J. Xiong, X. Feng, J. Xue, Y. Wang, H. Niu, Y. Gu, Q. Jia, Q. Wang and F. Yan, *Digital Discovery*, 2024, **3**, 1842–1851.

53 L. Van der Maaten and G. Hinton, *J. Mach. Learn. Res.*, 2008, **9**, 2579–2605.

54 L. Van Der Maaten, *J. Mach. Learn. Res.*, 2014, **15**, 3221–3245.

55 A. C. Belkina, C. O. Ciccolella, R. Anno, R. Halpert, J. Spidlen and J. E. Snyder-Cappione, *Nat. Commun.*, 2019, **10**, 5415.

56 H. Sun, S. J. Mumby, J. R. Maple and A. T. Hagler, *J. Am. Chem. Soc.*, 1994, **116**, 2978–2987.

57 H. Sun, *Macromolecules*, 1995, **28**, 701–712.

58 A. P. Thompson, H. M. Aktulga, R. Berger, D. S. Bolintineanu, W. M. Brown, P. S. Crozier, P. J. in 't Veld, A. Kohlmeyer, S. G. Moore, T. D. Nguyen, R. Shan, M. J. Stevens, J. Tranchida, C. Trott and S. J. Plimpton, *Comput. Phys. Commun.*, 2022, **271**, 108171.

59 L.-H. Lin, J.-J. Li, Y.-X. Pan, F. Yan, Z.-H. Luo and Y.-N. Zhou, *ACS Appl. Mater. Interfaces*, 2025, **17**, 55347–55359.